Chladni Plate Inspired Benchmark

1 Introduction

Chladni plates produce beautiful patterns when excited by a vibrating source. These patterns result from 2D standing waves, visualized by pouring sand on the plate.

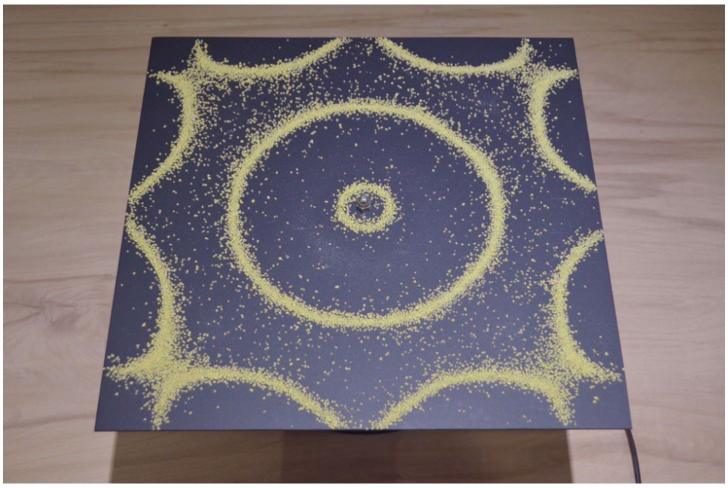

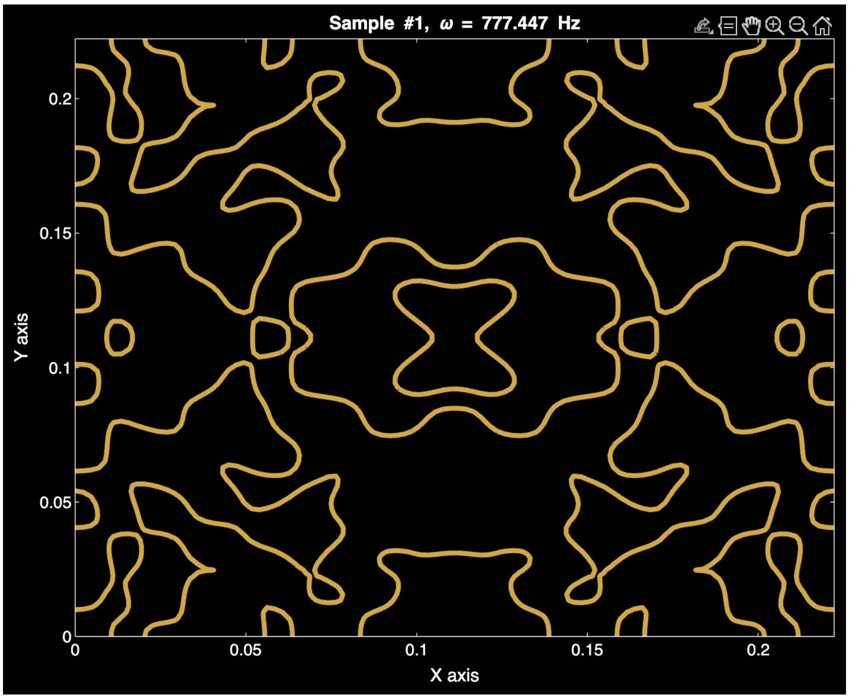

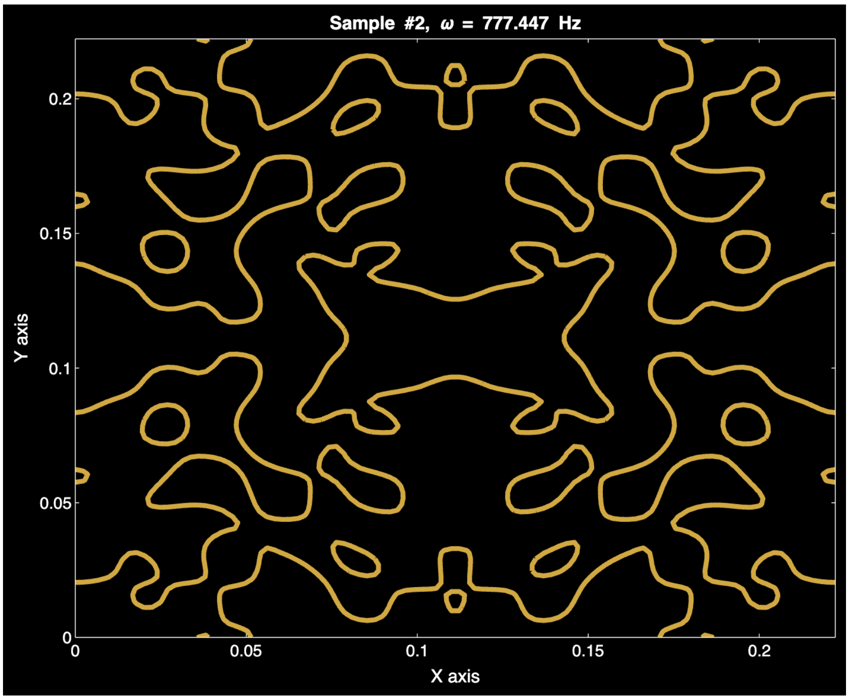

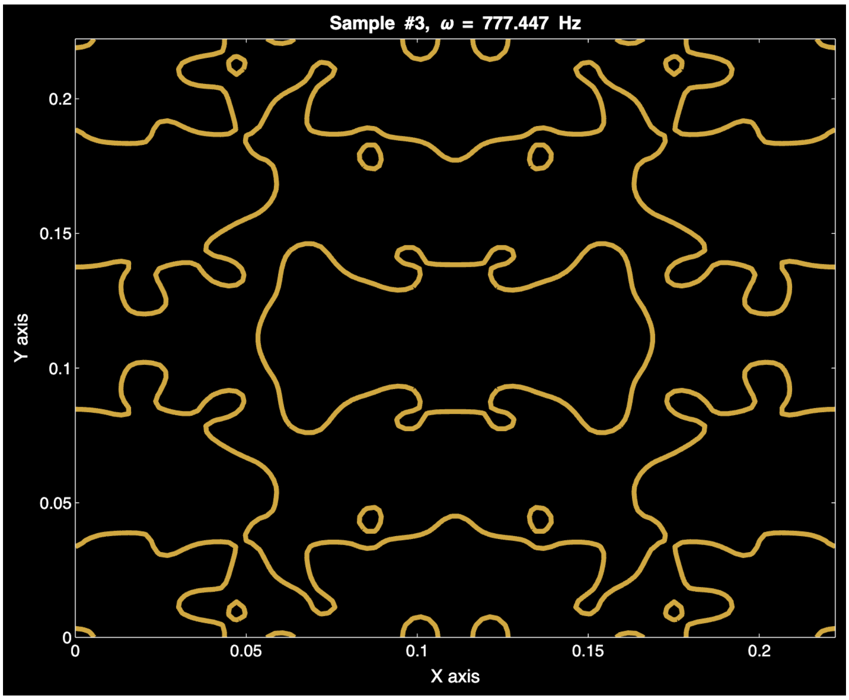

2 Mathematical Model

The 2D wave equation for the transverse displacement $u(x, y, t)$ is given by:

$$\frac{\partial^2 u}{\partial t^2} + \gamma \frac{\partial u}{\partial t} = \nu^2 \left(\frac{\partial^2 u}{\partial x^2} + \frac{\partial^2 u}{\partial y^2} \right) + S(x, y, t), \tag{1}$$

where:

- γ: Damping constant,

- ν: Transverse wave speed,
- $S(x, y, t)$: Driving force.

The driving force $S(x, y, t)$ is initially modeled as:

$$S(x, y, t) = s_0\, \delta\!\left(x - \tfrac{L}{2}\right) \delta\!\left(y - \tfrac{M}{2}\right) \cos(\omega t), \tag{2}$$

where δ is the Dirac delta function, s_0 is the source amplitude, and ω is the driving frequency.

2.1 Boundary and Initial Conditions

- **Boundary Conditions (Neumann):**

$$\frac{\partial u}{\partial n} = 0 \quad \text{on all edges}, \tag{3}$$

  which signifies zero normal slope (a "free edge" condition).

- **Initial Conditions:**

$$u(x, y, 0) = 0, \quad \frac{\partial u(x, y, 0)}{\partial t} = 0, \tag{4}$$

  meaning the plate starts from rest.

3 Solution Procedure

The solution involves the following steps:

3.1 Step 1: Eigenvalues and Eigenfunctions

For a rectangular plate of dimensions $L \times M$ and Neumann boundary conditions, the spatial eigenfunctions and eigenvalues satisfy:

$$\phi_{mn}(x, y) = \cos\!\left(\frac{m\pi x}{L}\right) \cos\!\left(\frac{n\pi y}{M}\right), \quad \lambda_{mn} = \nu^2 \left[\left(\frac{m\pi}{L}\right)^2 + \left(\frac{n\pi}{M}\right)^2\right]. \tag{5}$$

3.2 Step 2: Fourier Transform

Apply the (spatial) Fourier transform in x and y to convert spatial derivatives into algebraic expressions.

3.3 Step 3: Laplace Transform

Use the Laplace transform in time to handle the time derivatives. In the Laplace domain, one obtains:

$$s^2 \tilde{U} + \gamma s \tilde{U} + \lambda_{mn} \tilde{U} = \tilde{S}(s). \tag{6}$$

3.4 Step 4: Solve for $\tilde{U}$

$$\tilde{U}(s) = \frac{\tilde{S}(s)}{s^2 + \gamma s + \lambda_{mn}}. \tag{7}$$

3.5 Step 5: Inverse Laplace Transform

Take the inverse Laplace transform to recover the time-domain solution for each mode.

3.6 Step 6: Inverse Fourier Transform

Reconstruct the solution in physical space:

$$u(x,y,t) = \sum_{m,n} \frac{\phi_{mn}(x,y)\,\tilde{S}(s)}{\|\phi_{mn}\|^2\,\big(s^2+\gamma s+\lambda_{mn}\big)}. \tag{8}$$

4 Random Forcing Fields for Data-Driven Benchmarks

While a single delta-source at $(L/2, M/2)$ is common in classical derivations, certain data-driven or machine-learning applications require *many different* forcing fields as input. For instance, in *operator learning* (where we train a model to map an input function $S(x,y)$ to an output solution $u(x,y,t)$), a single δ-function forcing is insufficient to explore a broad range of boundary phenomena.

4.1 Definition of the Random Forcing

Instead of

$$S(x,y,t) = s_0\,\delta\big(x-\tfrac{L}{2}\big)\,\delta\big(y-\tfrac{M}{2}\big)\,\cos(\omega t),$$

we generate a more general, *random multi-mode* forcing of the form

$$S_k(x,y,t) \;=\; \sum_{m=1}^{M_{\max}}\sum_{n=1}^{N_{\max}} \alpha_{mn}^{(k)}\,\cos\!\Big(\frac{m\pi x}{L}\Big)\,\cos\!\Big(\frac{n\pi y}{M}\Big)\,f(t), \tag{9}$$

where:

- $\alpha_{mn}^{(k)}$ are *randomly sampled* coefficients for the k-th forcing realization,
- $M_{\max}, N_{\max}$ specify how many modes we include,
- $f(t)$ is some chosen time dependence (e.g., $\cos(\omega t)$ or a more complex function).

4.2 Motivation for Random Forcing

By introducing many different forcing patterns $S_k(x,y,t)$:

- We can generate *training datasets* for operator-learning or surrogate models, which learn a mapping $S(\cdot,\cdot) \mapsto u(\cdot,\cdot,t)$.
- This approach provides a broad set of input-output *examples*, better reflecting real-world scenarios where the driving force is not always localized at a single point.
- It allows us to explore how the plate responds to diverse spatial forcing fields, building a more generalizable model of the plate dynamics.